ANALYSIS AND EXPERIMENT ON SOLAR GREENHOUSE HEAT DEVICE INSULATION
/
太阳能温室加热装置保温性能分析与实验

Fu-cheng WANG*[1)], Chang-yin TIAN[1)], Bin-peng JIANG[2)], Ke-xin SUN[1)]
[1)] College of Engineering, Heilongjiang Bayi Agricultural University, Daqing, Heilongjiang / China
[2)] College of Civil and Hydraulic Engineering, Heilongjiang Bayi Agricultural University, Daqing, Heilongjiang / China
Corresponding author: Fu-cheng Wang
Tel:+8618645903113; E-mail:fuchengwang@byau.edu.cn
DOI: : https://doi.org/10.35633/inmateh-78-61

Keywords: *solar greenhouse, solar energy, heating device, numerical simulation*

ABSTRACT
This study proposes a solar energy collection and release device based on a matrix pipe system installed on the north wall of a solar greenhouse. The indoor thermal environment was analyzed theoretically, and finite element simulations using ANSYS were conducted, along with comparative experiments at the College of Engineering, Heilongjiang Bayi Agricultural University. The results showed good agreement between theoretical predictions, simulation results, and experimental data. The proposed device significantly enhances greenhouse thermal insulation and solar energy utilization efficiency, providing a useful reference for the application and dissemination of similar thermal storage systems in solar greenhouses.

摘要
本研究介绍了一种在太阳能温室北墙采用矩阵管系统的太阳能集热与释热装置。对室内热环境进行了理论分析，并在黑龙江八一农垦大学工程学院进行了基于 ANSYS 的有限元模拟和对比实验。理论和模拟的温度趋势与实验数据吻合良好。该装置显著提高了温室的保温性能和太阳能利用效率，为类似蓄热系统在太阳能温室中的应用和推广提供了有价值的参考。

INTRODUCTION
As key facilities overcoming geographical and seasonal limitations in traditional agriculture, solar greenhouses play a vital role in enabling winter production of fruits and vegetables in northern China, effectively alleviating seasonal supply shortages *(Zhiyuan et al., 2025)*. Conventional solar greenhouse walls, functioning as passive heat storage and release units, often exhibit insufficient heat dissipation during low-temperature nights, leading to inadequate thermal support for nocturnal crop growth *(Jin et al., 2019).* Enhancing heat storage and release capacity to improve nighttime indoor temperatures has thus become a critical research focus. The integration of solar heat collection and release systems presents a promising approach to advancing thermal performance while promoting energy conservation and emissions reduction.

Substantial research has been conducted globally to optimize the thermal performance of solar greenhouse walls. Regarding active heat storage-release systems, A roof truss pipe water circulation system was designed, which raised the average minimum nighttime temperature by 2.4°C, significantly improving thermal conditions (*Chengwei et al., 2016*). By evaluating three water-based heat storage systems, the results show that the performance of the solar collector system is superior to that of the traditional brick wall, highlighting the potential of water medium as an alternative to the wall (*Ying et al., 2020*). An active heat storage wall with a gravity-driven circulation pipe was proposed, simulation results confirmed that this heat storage wall can effectively increase the night temperature, reduce the heat load, and stabilize the thermal environment for crop growth (*Jinxuan et al., 2024*). By integrating active water storage bags, the insulation performance of greenhouses can be enhanced under various weather conditions (*Tuerhong et al., 2025*). A passive solar device was developed through parameter simulation, and the optimal configuration of the solar greenhouse could be determined through energy consumption analysis (*Abedini et al., 2024*).

Fu-cheng Wang, Assoc. Prof, Ph.D.; Changyin-Tian, MSc Ag; Bin-peng Jiang, MEng; Kexin-Sun, MSc Ag.

Existing studies have established the effectiveness of active heat storage-release systems in improving thermal environments and underscored the feasibility of water-based media, laying a technical foundation for solar energy applications in greenhouses. However, most prior work has centered on performance tests or simulations of individual systems, with limited comprehensive research integrating theoretical derivation, finite element simulation, and experimental validation of solar heat collection-release devices. This study deploys piping from a solar heat collection-release system on the north wall of a solar greenhouse, utilizing hot water circulation for nocturnal heat release. Finite element software is employed to simulate and compare the thermal behavior of greenhouses with and without the system. Through experimental monitoring of indoor and back-wall temperatures, this paper analyzes temperature variation patterns, evaluates improvements in nighttime insulation, and assesses solar energy utilization efficiency, thereby providing theoretical and practical insights for implementing solar heat collection-release systems in solar greenhouses.

MATERIALS AND METHODS

Model for Calculating Air Temperature in Solar Greenhouses

Assuming the solar greenhouse as a hollow cavity and neglecting radiative heat transfer from supporting structures, the heat exchange process of indoor air primarily involves thermal interactions with the inner surface of the plastic film, the soil surface, and the inner surface of the rear wall, as well as heat exchange with outdoor air induced by ventilation. The thermal balance equation can be expressed by Equation (1) *(Ping et al., 2022)*.

$$C_i \frac{dT_i}{d\tau} = h_c A_c (T_c - T_i) + h_{S1} A_{S1} (T_{S1} - T_i) + h_{B1} A_{B1} (T_{B1} - T_i) + h_{R1} A_{R1} (T_{R1} - T_i) + \frac{L \rho_i c_{p,i}}{3600} (T_o - T_i) \quad (1)$$

where:

C_i denotes the thermal capacity of indoor air (J/K); h_c represents the convective heat transfer coefficient between the plastic film and indoor air (W/(m²·K)); A_c is the area of the plastic film (m²); T_c indicates the inner surface temperature of the plastic film (K); h_{S1} refers to the convective heat transfer coefficient between the soil surface and indoor air (W/(m²·K)); A_{S1} stands for the surface area of the topsoil (m²); T_{S1} signifies the temperature of the topsoil (K); A_{B1} corresponds to the interior surface area of the wall (m²); T_{B1} denotes the surface temperature of the interior wall (K); h_{R1} indicates the convective heat transfer coefficient between the interior surface of the rear slope and indoor air (W/(m²·K)); A_{R1} represents the interior surface area of the rear slope; T_{R1} is the inner surface temperature of the rear slope (K); ρi refers to the density of indoor air (kg/m³); $c_{p,i}$ denotes the specific heat capacity of indoor air at constant pressure (J/(kg·K)); L symbolizes the ventilation rate, expressed as $L = NVi$ (where N is the air exchange rate, in exchanges per hour, and Vi is the volume of indoor air, in m³), in m³/h.

Thermal Modeling of Wall Temperature in Solar Greenhouses

The thermal transfer process of the rear wall in a solar greenhouse involves the following mechanisms: radiative heat exchange between the inner surface of the rear wall and the inner surfaces of the plastic film, soil, and rear slope; convective heat transfer between the inner surface of the rear wall and the indoor air; thermal conduction between the inner and outer surfaces of the rear wall; convective heat exchange between the outer surface of the rear wall and the outdoor air; and radiative exchange between the outer surface of the rear wall and the sky. Consequently, the thermal balance relationship and heat transfer governing equations can be expressed by Equations (2) to (4) *(Anzhe et al., 2024; Weiwei et al., 2021)*.

Thermal equilibrium at the inner surface is expressed as follows:

$$C_{B1} \frac{dT_{B1}}{d\tau} = \beta_{B1c} A_c (T_c - T_{B1}) + \beta_{S1B1} A_{S1} (T_{S1} - T_{B1}) + \beta_{R1B1} A_{R1} (T_{R1} - T_{B1}) + h_{B1} A_{B1} (T_i - T_{B1}) + Q_{B1B2} \quad (2)$$

The governing equation for heat transfer within the intermediate layer is as follows:

$$C_{B2} \frac{dT_{B2}}{d\tau} = Q_{B3B2} - Q_{B1B2} \quad (3)$$

The thermal equilibrium equation for the external surface is expressed as:

$$C_{B3} \frac{dT_{B3}}{d\tau} = \beta_{B3sky} A_{B3} (T_{sky} - T_{B3}) + h_{B3} A_{B3} (T_o - T_{B3}) + Q_{B3B2} \quad (4)$$

where:

C_{B1} denotes the thermal capacity of the surface wall layer, J/K; β_{B1c} represents the radiative heat transfer coefficient between the wall surface and the inner surface of the plastic film, W/(m²·K);

β_{S1B1} indicates the radiative heat transfer coefficient between the wall surface and the inner surface of the soil, W/(m²·K); β_{R1B1} signifies the radiative heat transfer coefficient between the inner surface of the wall and the inner surface of the rear slope, W/(m²·K); Q_{B1B2} corresponds to the heat transfer from the intermediate wall layer to the inner wall layer, W; C_{B2} refers to the thermal capacity of the intermediate wall layer, J/K; T_{B2} is the temperature of the intermediate wall layer, K; Q_{B3B2} describes the heat transfer from the outer wall layer to the intermediate wall layer, W; C_{B3} stands for the thermal capacity of the outer wall layer, J/K; T_{B3} indicates the temperature on the exterior side of the wall, K; β_{B3sky} represents the radiative heat transfer coefficient between the outer wall surface and the sky, W/(m²·K); T_{sky} denotes the effective sky temperature, K; A_{B3} specifies the outdoor-side surface area of the wall, m².

Diurnal Heat Collection Performance of Solar Thermal Collector Systems

Based on data such as water density and temperature variations at different time intervals, the total heat collection capacity (J) of the solar thermal collection and release system during operation can be calculated using the following expression *(Ren et al., 2019)*:

$$Q_c = \sum_{T_2}^{T_1} \rho_w C_w V (T_{t+1} - T_t) \quad (5)$$

The total solar radiation incident upon the surface of a solar energy collection and release device is defined as J, with its expression given by:

$$Q_I = \Delta t A \sum_{t_0}^{t_1} I_P \quad (6)$$

where:

ρ_W is the density of water, kg·m^{-3}; C_W is the specific heat capacity of water, J/K; V is the water storage volume, m³; T_t and T_{t+1} are the water temperatures of the heat collection device, °C; t_0 and t_1 are the start and end times of the system operation during the day respectively, h; A is the total area of the heat collection device, m²; I_p is the instantaneous solar irradiance on the surface of the heat collection device, W·m^{-2}; Δt is the time interval, s.

Through computational analysis, it is determined that the reservoir capacity of a solar greenhouse equipped with a heat collection and release system can be standardized at 1.5–2.5 m³ per 100 m² of greenhouse floor area *(He et al., 2025; Han et al., 2024)*. Taking a 240 m² solar greenhouse as an example, a reservoir with a capacity of 4–6 m³ can be configured. Assuming a water temperature variation range of 10°C, the corresponding heat storage and release capacity amounts to 167–251 MJ.

Nocturnal Heat Dissipation Capacity of Solar Thermal Collector Systems

The thermal energy storage and release unit can be functionally characterized as a heat sink, with the nocturnal heat flux Q_h (W) released into the greenhouse expressed as *(Xinge et al., 2023)*:

$$Q_h = K_P F_p (t_w - t_i) \quad (7)$$

where: the heat transfer coefficient for the north wall array-configured pipelines, denoted as K_p, is expressed in W/(m²·K). Based on extrapolation from relevant literature *(Zhong et al., 2025)*, it can be approximated as 9 W/(m²·K). F_p represents the surface area of the pipelines in square meters.

Taking a 240 m² solar greenhouse as an example, this study employs pipelines with an inner diameter of 25 mm and an outer diameter of 33.5 mm. The average external surface area per meter of pipeline is approximately 0.1 m². With an effective heat dissipation length of 2 m per column in the matrix pipeline arrangement, the surface area for heat dissipation per column amounts to 0.2 m². By arranging the pipes at a spacing of 0.2 m, the total heat dissipation area of the solar energy collection and release system reaches approximately 40 m². Although the water temperature in the solar energy collection and release system may remain relatively low after daytime thermal storage, the substantial total heat dissipation area of the system enables significant heat release. Calculations for the 240 m² solar greenhouse indicate that, with an indoor-to-water temperature difference of 8°C, the nighttime heat flux of the solar energy collection and release system can still achieve 2.9 kW.

Theoretical Analysis of the Nocturnal Heating Effect of Solar Thermal Collector Systems

For the solar greenhouse with parameters established in this study, employing a thermal insulation quilt with a heat transfer coefficient of approximately 1 W/(m²·°C), the required heating flux density to raise the indoor temperature by 1°C is 3–4 W/m², and the average nightly heating requirement is 110–130 kJ/m². Taking a 240 m² solar greenhouse as an example, a theoretical analysis of the nighttime heating performance is conducted from two aspects: the heat storage and dissipation capacities of the solar heat collection and release system.

In the heat storage capacity calculation, with a heating flux density of 3–4 W/m² needed per 1°C increase in indoor temperature and an average nightly heating requirement of 110–130 kJ/m², the total heating demand for the entire greenhouse amounts to 26.4–31.2 MJ. Given that the water-based thermal storage unit of the aforementioned system can achieve a heat storage and release capacity of 167–251 MJ, and considering the influence of weather conditions, a stable daily heat release of 80 MJ is adopted for calculation. This can raise the indoor air temperature by approximately 2.6°C.

In the heat dissipation capacity calculation, the heating flux required to increase the indoor temperature by 1°C is 3–4 W/m², corresponding to a heating power input of about 0.7 kW per 1°C rise. Based on the total thermal power output of the solar heat collection and release system being 2.9 KW, the indoor air temperature can be elevated by approximately 2.9°C. Therefore, according to theoretical calculations, the solar heat collection and release system exhibits satisfactory nighttime heating performance, capable of increasing the greenhouse indoor temperature by about 2.7°C.

Development of Finite Element Model for Solar Greenhouse

To investigate the thermal insulation performance dynamics of a solar energy collection and release system in a solar greenhouse, a conventional wall-structured solar greenhouse was selected as the control. Finite element simulation analysis was conducted, with both the experimental greenhouse equipped with the solar energy system and the control greenhouse modeled at the College of Engineering, Heilongjiang Bayi Agricultural University (46°35′N, 125°09′E). The simulation adhered to the specifications outlined in *Protected Horticulture* by Professor Gao Lihong of China Agricultural University *(Tianyang et al., 2023)*. Both greenhouses were oriented east–west, facing south, with a length of 40 m, a span of 6 m, and a ridge height of 3.2 m, as illustrated in Fig. 1. The total numbers of mesh elements were 283,140 and 590,243, respectively, with orthogonal quality values approximating 0.8, meeting computational requirements. The material properties of the solar greenhouse models are summarized in Table 1.

(a)Grid division of common wall solar greenhouses

(b)Grid division of solar heat collection and release device solar greenhouse

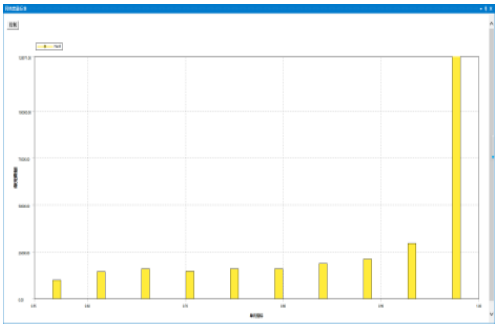

(a)Orthogonal quality of common wall solar greenhouses

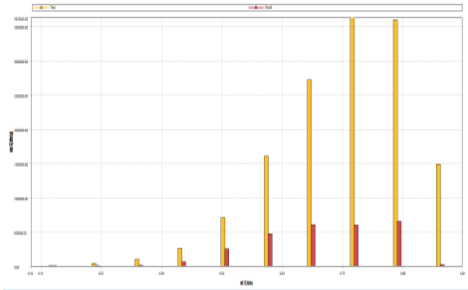

(b)Orthogonal quality of solar heat collection and release device solar greenhouse

Fig. 1 – Model diagram of solar greenhouse

Table 1

Parameters of thermal properties of solar greenhouse materials

Building envelope	Materials	Density [kg/m³]	Pyrocon-ductivity [J/(kg·K)]	Specific heat capacity [W/(m·K)]	Thickness [m]	Absorption factor of solar radiation
North wall	Clay bricks	1800	0.81	1050	0.34	
Soil	Soil	1900	1.518	840		0.9
Back slope	Red brick	1650	0.62	840	0.2	0.6
	Asbestos tile	600	0.15	760	0,07	0.6
Cover material	PE film	1360	0.15	1050	0.002	
Textile category	Quil	400	0.08	820	0.04	

Governing equation

Within greenhouse environments, an internal thermal equilibrium is maintained through the synergistic interactions of three heat transfer mechanisms: conduction, convection, and radiation. These processes, encompassing both heat transfer and fluid flow, adhere to fundamental physical conservation laws *(Guangyu et al., 2022; Wang et al., 2024; Jianwei et al., 2025)*. Accordingly, this study is grounded in the principles of mass conservation, momentum conservation, and energy conservation.

Boundary Condition Specification

The cladding system employs semi-transparent boundaries, with the effective sky temperature designated as the external radiative temperature of the cover layer, thereby neglecting radiative heat exchange with the surrounding environment (*Qiangwei et al., 2024; Xinyi et al., 2024)*. The north wall and north slope exterior surfaces are subjected to convective heat transfer boundary conditions. As the diurnal temperature variation of soil below 0.55 m depth is negligible, the soil at 0.6 m underground is defined as the thermal boundary, utilizing measured temperature values. Given that the east-west span of the greenhouse significantly exceeds its north-south span, and the surface area of the east and west walls is relatively small compared to other enclosure structures, heat dissipation through these walls is disregarded and adiabatic boundary conditions are applied accordingly (*Xuejiao et al., 2016)*.

Turbulence model and radiation model

The nocturnal temperature field within a solar greenhouse constitutes a transient process (*Jingtao et al., 2024)*. The greenhouse interior can be characterized as a natural convection scenario within an enclosed space, typically assessed using the Rayleigh number (Ra). A turbulent regime is identified when Ra exceeds 10; consequently, the k-ε turbulence model is employed for simulation. To achieve enhanced computational accuracy, the present study utilizes the Realizable k-ε turbulence model, incorporates boundary-layer grid refinement, and applies the enhanced wall treatment method (*Xinge et al., 2023)*. Additionally, the discrete ordinates (DO) radiation model is implemented, with solar ray tracing activated during simulation. Relevant parameters such as simulation duration and geographical location are also prescribed.

Comparative Analysis of Diurnal Temperature Variations in Greenhouses

As illustrated in Fig. 2, between 23:00 and 08:00, both greenhouses exhibited minimal temperature fluctuations, with the greenhouse equipped with a solar heat collection and release system maintaining temperatures 0.8–1.6 ℃ higher than the conventional greenhouse. The average indoor-outdoor temperature differential increased by 1.2 ℃ during the night, and thermal retention efficiency improved by approximately 18%, attributable to enhanced nighttime insulation through heat exchange via the piping system carrying heated water. After 08:00, solar radiation intensified, causing both greenhouse types to warm. However, the warming rate of the equipped greenhouse was 2.1 ℃/h, lower than the 2.4 ℃/h observed in the conventional greenhouse, owing to higher indoor humidity levels following system deactivation, which moderated heat absorption. Daily peak temperatures occurred between 13:00 and 15:00, with the peak delayed by approximately one hour in the equipped greenhouse due to the thermal storage and release by the water in the piping system. During the subsequent cooling phase, the equipped greenhouse exhibited a cooling rate of 1.3 ℃/h, slower than the 1.5 ℃/h rate of the conventional greenhouse, as a result of heat release from the hot water in the north-wall pipes. Based on the thermal balance model, the system contributed approximately 27% to nighttime heat exchange, confirming its role in actively regulating the indoor thermal environment and effectively enhancing the thermal performance of the solar greenhouse.

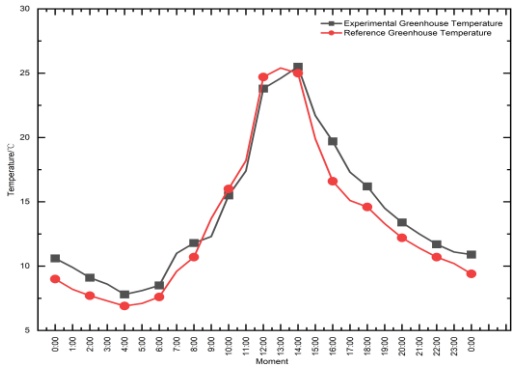

Fig. 2 – Finite element simulated diurnal temperature variation in a solar greenhouse

Comparative Analysis of Temperature Field Variations

Given that the length of the solar greenhouse is approximately seven times its span, the influence along the longitudinal dimension is relatively minor. Therefore, a two-dimensional cross-sectional temperature field was selected for analysis. As illustrated in Fig. 3, the temperature distribution reveals the following observations:

1) At 23:00, the solar heat collection and release system operates in heat release mode, raising the indoor temperature by 1.2 °C compared to a conventional greenhouse. By 02:00, as the heat release capacity of the system gradually diminishes with increasing cumulative heat dissipation, the temperature difference between the two greenhouse configurations peaks at 1.6 °C. During the period from 05:00 to 08:00, with a deceleration in the heat release rate, the average temperatures of the two greenhouse types converge and begin to rise gradually under the influence of solar radiation.

2) From 23:00 to 08:00, the temperature contour plots exhibit similar patterns across different time points. The wall integrated with the solar heat collection and release system transfers heat indoors, causing the indoor air to rise along the rear wall. The warm airflow follows an arched downward path upon encountering the cooler southern wall surface, is reheated when passing over the ground, and thereby establishes a circulation pattern within the greenhouse. This mechanism elevates the average indoor temperature by 0.8–1.6 °C relative to a conventional solar greenhouse with a standard wall, effectively maintaining higher nighttime temperatures.

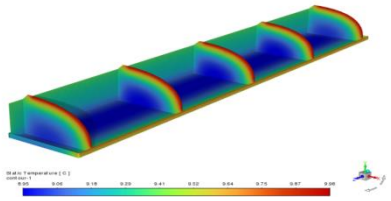

23:00 Temperature Distribution Diagram of Standard Wall Solar Greenhouse

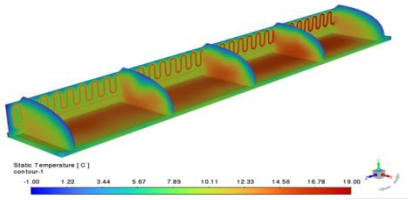

23:00 Temperature Distribution Diagram of Solar Thermal Storage Wall in Solar Greenhouse

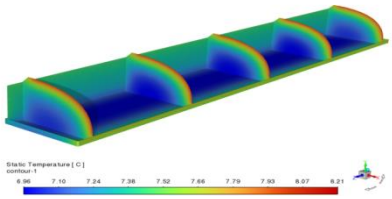

02:00 Temperature Distribution Diagram of Standard Wall Solar Greenhouse

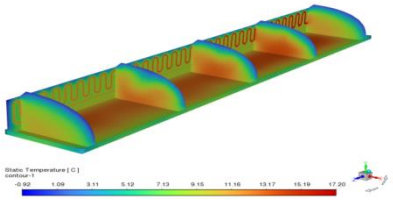

02:00Temperature Distribution Diagram of Solar Thermal Storage Wall in Solar Greenhouse

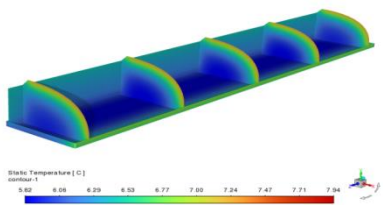

05:00 Temperature Distribution Diagram of Standard Wall Solar Greenhouse

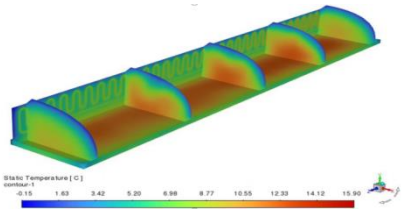

05:00Temperature Distribution Diagram of Solar Thermal Storage Wall in Solar Greenhouse

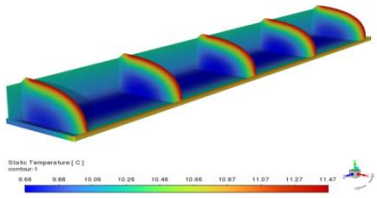

08:00 Temperature Distribution Diagram of Standard Wall Solar Greenhouse

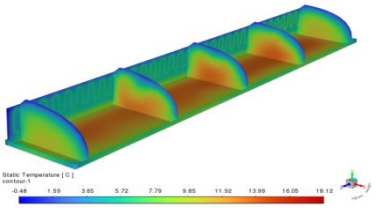

08:00Temperature Distribution Diagram of Solar Thermal Storage Wall in Solar Greenhouse

Fig. 3 – Temperature distribution map of solar greenhouse

Overview of the Experimental Site

To validate the accuracy of finite element simulations, experimental tests were conducted on both the internal and external environments of the greenhouse. The experimental solar greenhouse is located in Daqing City, Heilongjiang Province (46°35'N, 125°09'E). The measured total solar radiation value is compared with the theoretical clear-sky solar radiation of the same day, a clear-sky index greater than 0.6 is defined as a sunny day, and a clear-sky index less than or equal to 0.6 is defined as a cloudy day. The measured greenhouse temperature data were compared with the simulation results, to verify its changes in fact. For experimental convenience, as illustrated in Fig. 4, the span and ridge height of the test platform were scaled according to the reference greenhouse dimensions, (a) is the control group, and (b) is the experimental group. The structural parameters of the solar greenhouse are presented in Table 2.

(a)Conventional Wall-Style Solar Greenhouse

(b)Solar Thermal Collection and Release System for Sunlight Greenhouse

Fig. 4 – Scale drawing of solar greenhouse

Table 2

Structure parameters of solar greenhouse

Length (m)	Span (m)	Height (m)	Back-roof angle (°)	Backwall	
				Height (m)	Thickness (m)
2	1.5	1	30	0.8	0.2

RESULTS

Indoor Temperature Variations Under Typical Weather Conditions

According to Yiming Li et al., verified that the water circulation system of solar heat collection panels has the optimal heat storage and release capacity. This system operates well and is highly adaptable, and it has great potential to replace the traditional brick wall heat storage body in solar greenhouses (*Yiming et al., 2023*).

A comparative experiment was conducted during a typical clear period from November 5 to 7, 2024. As illustrated in Fig. 5, the temperature inside the experimental greenhouse was generally higher than that of the control group throughout the day. At 08:00 when the thermal insulation cover was removed, the indoor temperatures were 9.6°C and 9.2°C for the experimental and control groups, respectively. From 08:00 to 13:00, the indoor temperature rose rapidly with increasing solar irradiance. Around 09:00, the control group exhibited a temporarily higher temperature than the experimental group, likely due to its higher humidity. Both groups reached their daily maximum temperatures around 13:00, with the experimental group at 20.7°C and the control group at 19.8°C. During this period, the average temperature difference was 0.2°C, with a maximum of 0.9°C. From 13:00 to 23:00, as solar radiation weakened, indoor temperatures decreased. After the thermal insulation cover was reapplied at 16:00, the rate of temperature decline slowed. The average temperature difference during this phase was 0.4°C, with a maximum of 1.2°C.

Between 23:00 and 08:00, the heat storage and release system was activated. The average nighttime temperatures for the experimental and control groups were 5.6°C and 5.0°C versus 4.3°C and 3.9°C, respectively, resulting in an average difference of 1.2°C and a maximum of 2.0°C, attributable to heat released by hot water circulation in the north wall pipes. The results indicate that the system increased the average nighttime indoor temperature of the solar greenhouse by 1.3°C during the trial period.

A comparative experiment was conducted during a typical overcast period from November 19 to 21, 2024. As shown in Fig. 6, when the thermal blanket was removed at 8:00, the indoor temperatures of the experimental and control groups were 7.2°C and 6.6°C, respectively. With a gradual increase in solar irradiance in the morning, the indoor temperatures rose via heat exchange through the building envelope. Both greenhouse types reached their daily peaks around 12:00, with the experimental group at 15.9°C and the control group at 15.0°C, yielding an average temperature difference of 0.38°C and a maximum difference of 1.0°C. The earlier peak was attributed to insufficient total solar radiation on cloudy days. In the afternoon, as solar radiation diminished, indoor temperatures decreased. At 16:00, the thermal blankets were deployed to minimize heat loss. During this phase, the average temperature difference between the two groups was 0.58°C, with a maximum of 1.5°C. The heat charge-discharge system was activated at 23:00; however, limited solar irradiation on cloudy days resulted in lower water temperatures. The nighttime average temperatures for the experimental group were 3.9°C and 3.8°C, compared to 3.1°C and 2.9°C for the control group, corresponding to an average difference of 0.8°C and a maximum difference of 1.4°C. The results indicate that the solar thermal charge-discharge system increased the average nighttime indoor temperature by 0.8°C under overcast conditions, though its thermal retention effect was less pronounced compared to clear days.

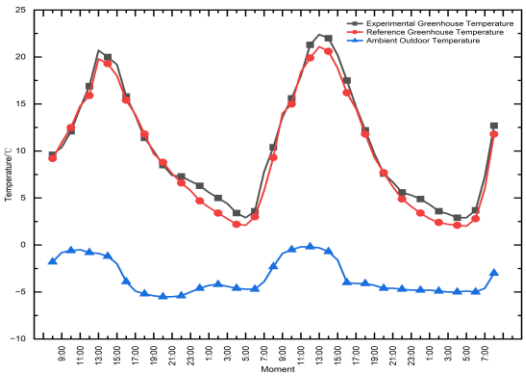

Fig. 5 – Indoor and outdoor temperatures on a typical sunny day

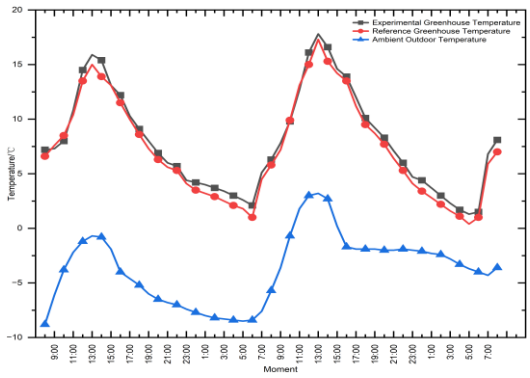

Fig. 6 – Indoor and outdoor temperatures on a typical cloudy day

Temperature Variation Patterns of the Rear Wall under Typical Weather Conditions

Fig.7 illustrates that the temperature variation trends of the back wall in both the experimental and control greenhouses are consistent, while the regulatory effect of the device on wall temperature varies with weather conditions. During typical sunny days (November 5–7), the peak back-wall temperatures in the experimental greenhouse occurred at 13:00, reaching 20.9°C and 21.8°C, which were 0.9°C and 1.1°C higher than those in the control greenhouse, respectively. The temperature difference between the two groups remained minimal from 08:00 to 23:00, except for a brief period around 10:00 when the wall temperature of the control greenhouse temporarily exceeded that of the experimental group. This anomaly was attributed to the absorption of solar radiation by residual water in the north-wall pipes of the experimental group. During the device operation period from 23:00 to 08:00, the average back-wall temperature in the experimental greenhouse reached 5.5°C, representing a 1.4°C increase compared to the control greenhouse. Under typical overcast conditions (November 19–21), influenced by reduced solar radiation and shorter daylight duration, the peak back-wall temperature occurred one hour earlier than on sunny days. From 23:00 to 08:00, the average back-wall temperature in the experimental greenhouse was 3.9°C, which was 0.6°C higher than that in the control greenhouse. The solar heat collection and release system exhibits significant thermal storage capacity, enabling supplemental heating by releasing stored heat via hot water circulation into the interior (including the wall) during nighttime. Moreover, abundant solar radiation on sunny days results in higher heat accumulation in the device, leading to a more pronounced improvement in wall temperature compared to overcast conditions.

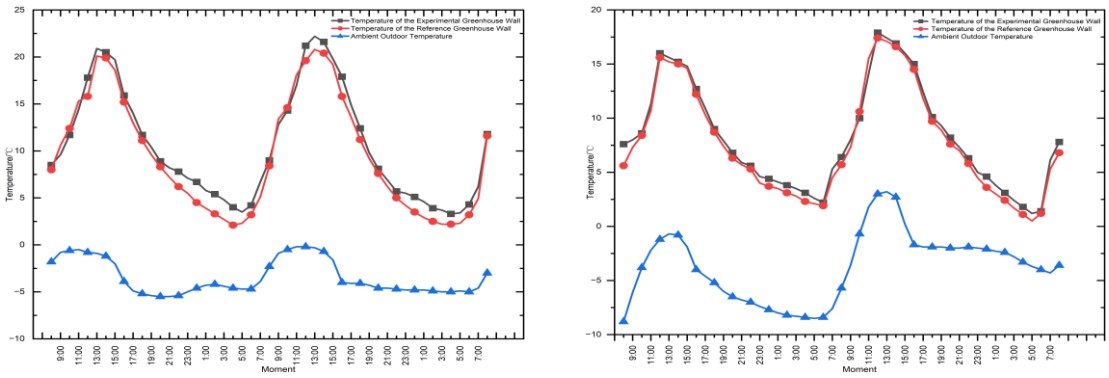

(a) Rear wall temperature on a typical sunny day **(b) Rear wall temperature on a typical cloudy day**

Fig. 7 – Variation in rear wall temperature of solar greenhouse under typical weather conditions

Effective Diurnal Accumulated Temperature in Solar Greenhouses

Effective accumulated temperature refers to the total heat required for a crop in a greenhouse to complete a certain developmental stage. As illustrated in Figure 7, under typical weather conditions, the solar heat collection and release-equipped greenhouse attained a maximum daily effective accumulated temperature of 137.4 °C·h on November 6 and a minimum of 67.7 °C·h on November 19, averaging 103.1 °C·h. In comparison, the reference wall-body greenhouse recorded corresponding values of 127.3 °C·h (maximum), 60.9 °C·h (minimum), and an average of 94.6 °C·h during the same period. Throughout the four-day observation, the solar-equipped greenhouse consistently maintained higher daily effective accumulated temperatures than the reference greenhouse, with differentials ranging from 5.6 °C·h (minimum) to 12.7 °C·h (maximum), averaging 8.5 °C·h. Compared to the conventional wall structure, the implemented system enhances the interior's daily effective accumulated temperature by 8.9%, thereby providing more favorable growth conditions for greenhouse flora.

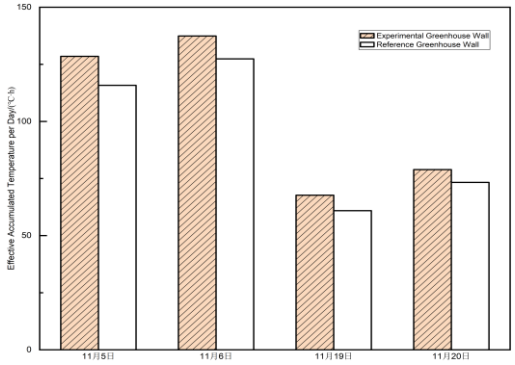

Fig. 8 – Daily effective accumulated temperature

CONCLUSIONS

(1) Theoretical calculations indicate that each 1°C increase in indoor temperature requires a heating flux density of 3–4 W/m². From the perspective of heat storage capacity, with a daily heat release of 80 MJ, the device can raise the indoor temperature by 2.6°C. Based on heat dissipation capacity, the total heat flux of the device is 2.9 kW, which can increase the indoor temperature by 2.9°C. The solar heat collection and release system elevates the average indoor temperature by approximately 2.7°C, demonstrating the device's effective thermal retention performance during nighttime.

(2) Finite element simulation results reveal that, during nighttime, the indoor temperature of a solar greenhouse equipped with a solar heat collection and release device is 0.8–1.6°C higher than that of a conventional wall-structured solar greenhouse, indicating superior thermal insulation performance of the former.

(3) Comparative experiments under typical weather conditions show that, relative to a conventional wall, the solar heat collection and release wall exhibits temperature differences of 1.4°C on sunny days and 0.6°C on cloudy days. The average nighttime temperature differences are 1.3°C and 0.8°C for sunny and cloudy conditions, respectively. Compared to the control wall, the effective accumulated temperature difference averages 8.5°C·h per day, representing an 8.9% improvement in effective indoor accumulated temperature. These findings confirm the enhanced nighttime thermal retention capability of the solar heat collection and release system.

Theoretical calculations and simulation results exhibit a trend highly consistent with experimental data, indicating that the solar energy collection and release system significantly enhances the thermal insulation performance of solar greenhouses. This improvement contributes to an increased utilization efficiency of solar energy resources, offering valuable insights for the practical application of such systems in solar greenhouse settings.

REFERENCES

[1] Abedini, H, M., Sarkardehi, E., Sabzevar B.H., (2024). Investigating Effective Parameters for Enhancing Energy Efficiency with an Attached Solar Greenhouse in Residential Buildings: A Case Study in Tabriz, Iran. *Asian Journal of Civil Engineering*, Vol. 26, pp. 1-15, America.

[2] Anzhe, Li, Hongjuan, Hou, Xi, Wang, (2024). Research on the Impact of Photovoltaic Module Layout on the Thermal and Light Environment of Photovoltaic Greenhouses (光伏组件布置方式对光伏温室温光环境的影响研究). *Acta Energiae Solaris Sinica*, Vol. 45, pp. 285-294, Beijing/China.

[3] Chengwei, Ma, Yichen, Jiang, Jieyu, Cheng, (2016). Analysis and Experiment on the Performance of Water Circulation System of Steel Pipe Network Formed by Roof Truss for Heat Collection and Release in Chinese Solar Greenhouse. *Editorial Office of Transactions of the Chinese Society of Agricultural Engineering*, Vol. 32, pp. 209-216, Beijing/China.

[4] Guangyu, Bai, Weidong, Zhuang, (2022). Thermal Environment Simulation of Multi-layer Covered Integrated Solar Greenhouse Based on CFD (基于CFD的多层覆盖一体式日光温室热环境模拟). *Transactions of the Chinese Society for Agricultural Machinery*, Vol. 44, pp. 218-227, Beijing/China.

[5] Han, F., Chen, C., Chen, H., (2024). Research on creating the indoor thermal environment of the solar greenhouse based on the solar thermal storage and release characteristics of its north wall. *Applied Thermal Engineering*, Vol. 241, Netherlands.

[6] He, M, Wan, X, Liu, H, (2025). Theory and application of sustainable energy-efficient solar greenhouse in China. *Energy Conversion and Management*, Vol. 325, Netherlands.

[7] Jianwei, Pang., Xi, Wang., Hongjuan, Hou., (2025). Research on the Impact of Solar Heat Collection and Storage Devices on the Thermal Environment of Prefabricated Solar Greenhouses (太阳能集热蓄热装置对装配式日光温室热环境影响研究). *Acta Energiae Solaris Sinica*, Vol. 46, pp. 470-478, Beijing/China.

[8] Jin, Sun, Hongbo, Gao, Jing, Tian, (2019). Current Situation and Trend of Facility Horticulture in China (中国设施园艺发展现状与趋势). *Journal of Nanjing Agricultural University*, Vol. 42, pp. 594-604, Nanjing/China.

[9] Jingtao, Wu, (2024). Research on the Thermal Insulation Performance of Rice Straw Ash Cement Mortar for Solar Greenhouse Walls (水稻秸秆灰水泥胶结料日光温室墙体保温性能研究). *Heilongjiang Bayi Agricultural University*, Heilongjiang/China.

[10] Jinxuan, Chen, Zhenyu, Du, (2024). Numerical Study on the Improvement of Thermal Environment in Solar Greenhouse by New Active Heat Storage and Release Wall (新型主动蓄放热墙体改善日光温室内热环境的数值研究). *Acta Energiae Solaris Sinica*, Vol. 45, pp. 431-440, Beijing/China.

[11] Yiming, Li, Yongxi, Li, Xiang, Yue, (2021). Experimental Study on Heat Storage and Release Performance of Water Medium Energy-saving Solar Greenhouse (水介质节能日光温室蓄放热性能试验). *Journal of Shenyang Agricultural University*, Vol. 52, pp. 306-313, Shenyang/China.

[12] Ping, Zou, Luyan, Jiang, Haoshu, Ling, (2022). Optimization Research on Thermal Properties of Phase Change Materials Applied to Solar Greenhouse Walls (应用于日光温室墙体的相变材料热物性优化研究). *Acta Energiae Solaris Sinica*, Vol. 43, pp. 139-147, Beijing/China.

[13] Qiangwei, Ma, Ming, Li, Lichun, Wang, (2024). Heat Storage and Release Characteristics of Combined Heat Storage System for Prefabricated Flexible Wall Solar Greenhouse (装配式柔性墙体日光温室联合储热系统蓄放热特性). *Transactions of the Chinese Society of Agricultural Engineering*, Vol. 40, pp. 183-193, Beijing/China.

[14] Ren, J., Zhao, Z., Zhang, J., (2019). Study on the hygrothermal properties of a Chinese solar greenhouse with a straw block north wall. *Energy & Buildings*, Vol. 193, pp. 127-138, Netherlands.

[15] Tianyang, X., Yiming, L., Zhouping, S., (2023). Performance study of an active solar water curtain heating system for Chinese solar greenhouse heating in high latitudes regions. *Applied Energy*, Vol.332, Netherlands.

[16] Tuerhong, A., Xu, H., Liu, H., (2025). Application Effect of Active Heat Storage and Release Water Bags in Solar Greenhouses in Hetian Region. *Asian Agricultural Research*, Vol. 17, pp. 17-22, USA.
[17] Wang, J., Luo, Q., Cheng, J., (2024). Study on thermal property of a solar collector applied to solar greenhouse. *Applied Thermal Engineering*, Vol. 244, Netherlands.
[18] Weiwei, X., Huiqing, G., Chengwei, M., (2021). An active solar water wall for passive solar greenhouse heating. *Applied Energy*, Vol. 308, Netherlands.
[19] Xinge, C., Hao, L., Gang, W., (2023). Coupled heat and humidity control system of narrow-trough solar collector and solid desiccant in Chinese solar greenhouse: Analysis of optical/thermal characteristics and experimental study. *Energy*, Vol. 273, Netherlands.
[20] Xinge, Chen, (2023). Research on Thermal and Humidity Regulation System of Solar Greenhouse Based on Concentrated Solar Collector (基于聚光式太阳能集热器的日光温室热湿调控系统研究). *Inner Mongolia University of Technology*, Neimenggu/China.
[21] Xinyi, Chen, (2024). Research on the Performance of Water Module Prefabricated Solar Greenhouse (水模块装配式日光温室性能研究). *Northwest A&F University*, Shanxi/China.
[22] Xuejiao, Tong., Zhouping, Sun., Tianlai, Li., (2016). Experimental Effects of Solar Water Circulation System in Solar Greenhouse in Winter and Summer (日光温室太阳能水循环系统冬季与夏季试验效果). *Acta Energiae Solaris Sinica*, Vol. 37, pp. 2306-2313, Beijing/China.
[23] Ying, Zhou., Shuangxi, Wang., Zhonghua, Liu., (2020). Simulation Research on Composite Phase Change Insulation Wall of Solar Greenhouse Based on ANSYS (基于ANSYS的日光温室复合相变保温墙体的模拟研究). *Acta Energiae Solaris Sinica*, Vol. 41, pp. 113-122, Beijing/China.
[24] Zhiyuan, Zhang., Yinbin, Zhu., Yubo, Guo., (2025). Distribution Characteristics of Light Environment in Flexible Insulated Solar Greenhouse and Improvement Measures (柔性保温日光温室光环境分布特征及改善措施). *Journal of China Agricultural University*, Vol. 30, pp. 197-205, Beijing/China.
[25] Zhong, C., Zhou, H., (2025). Effects of different ventilation speeds on the thermal environment of solar greenhouses. *INMATEH-Agricultural Engineering*, Vol. 76(2), pp. 441-450. Bucharest / Romania. DOI: https://doi.org/10.35633/inmateh-76-37